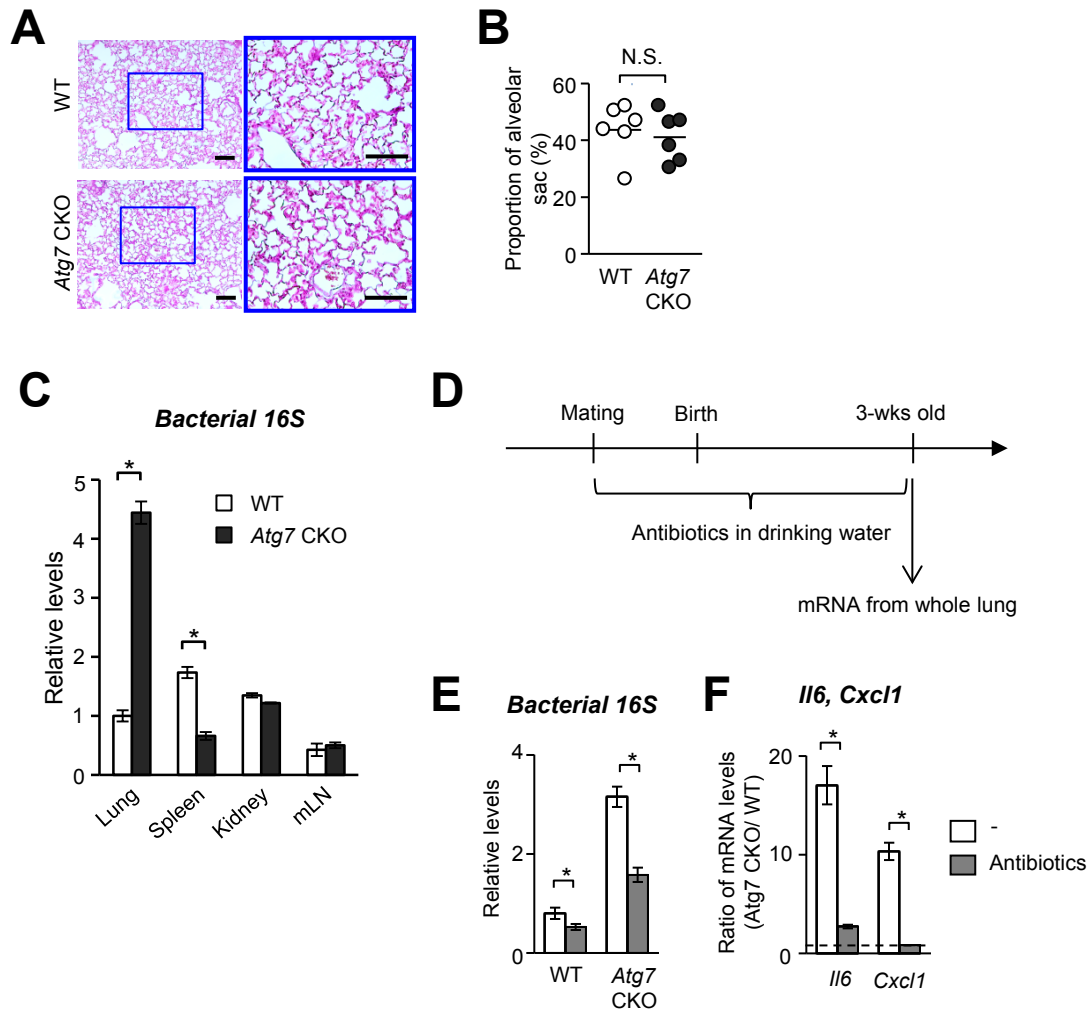


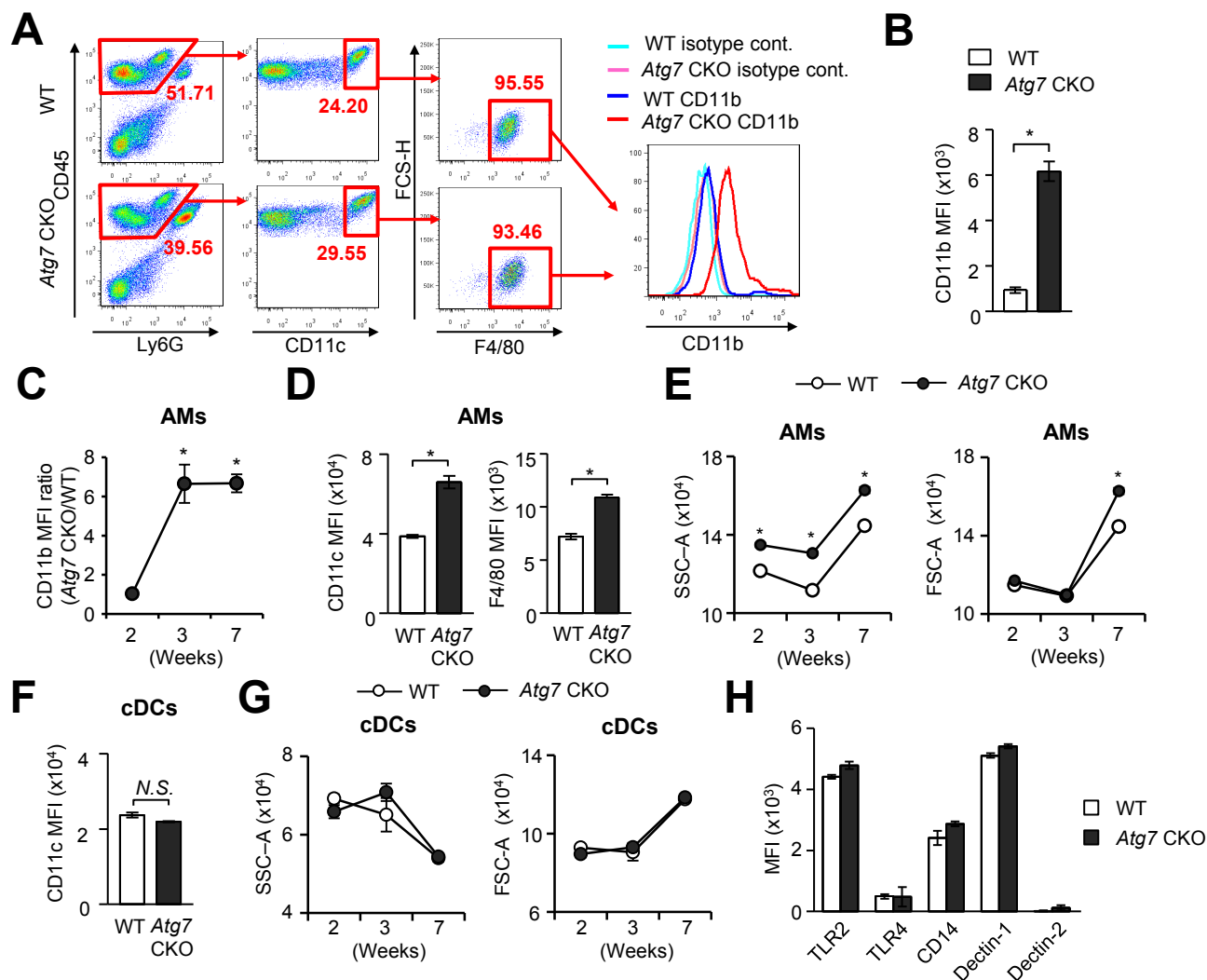
SUPPLEMENTARY FIGURE 1. Characterization of *Atg7* CKO mice, gating strategy of innate immune cells, and cellularity of adaptive immune cells in the lung. (A) Expression of *Atg7* was evaluated by qPCR. *Actb* was used as internal control. $n=4$ per group. Error bars represent mean \pm SD. (B) LC3 puncta formation in AMs, BMMs, BMDCs and PMNs. Cells were stimulated with LPS (100 ng/ml) for 1 hr and stained for DAPI (blue) and LC3 (green). Scale bars indicate 10 μ m. In (A) and (B), alveolar macrophages (AMs) were obtained from the lungs of naïve 7-wk old WT and *Atg7* CKO mice. BMMs and BMDCs were derived from BM with M-CSF and GM-CSF, respectively. PMNs were obtained from peritoneal cavity of 7-wk old WT and *Atg7* CKO mice 12 hr after thioglycollate injection. (C) Gating strategy of innate immune cells in the lung. Neutrophils were gated as CD11b⁺Ly6G⁺ cell population. Ly6C⁺ monocytes/macrophages were gated as CD11b⁺Ly6G⁻Ly6C⁺ population. (D) Alveolar macrophages and cDCs were gated as CD45⁺CD11c^{hi}F4/80⁺ and CD45⁺CD11c^{hi}F4/80⁻, respectively. (E) Expression of Siglec-F on the surface of alveolar macrophages. (F, G) Proportion (F) and cell numbers (G) of adaptive immune cells in the lung of 7-wk old *Atg7* CKO mice. Error bars represent mean \pm SD. N.S.; not significant. (H) LC3 puncta formation in AMs obtained from 3-wk old mice. AMs were stimulated with LPS (100 ng/ml) for 1 hr and stained for DAPI (blue) and LC3 (green). Scale bars indicate 5 μ m. Data are representative of four independent experiments.

Supplementary Figure 2



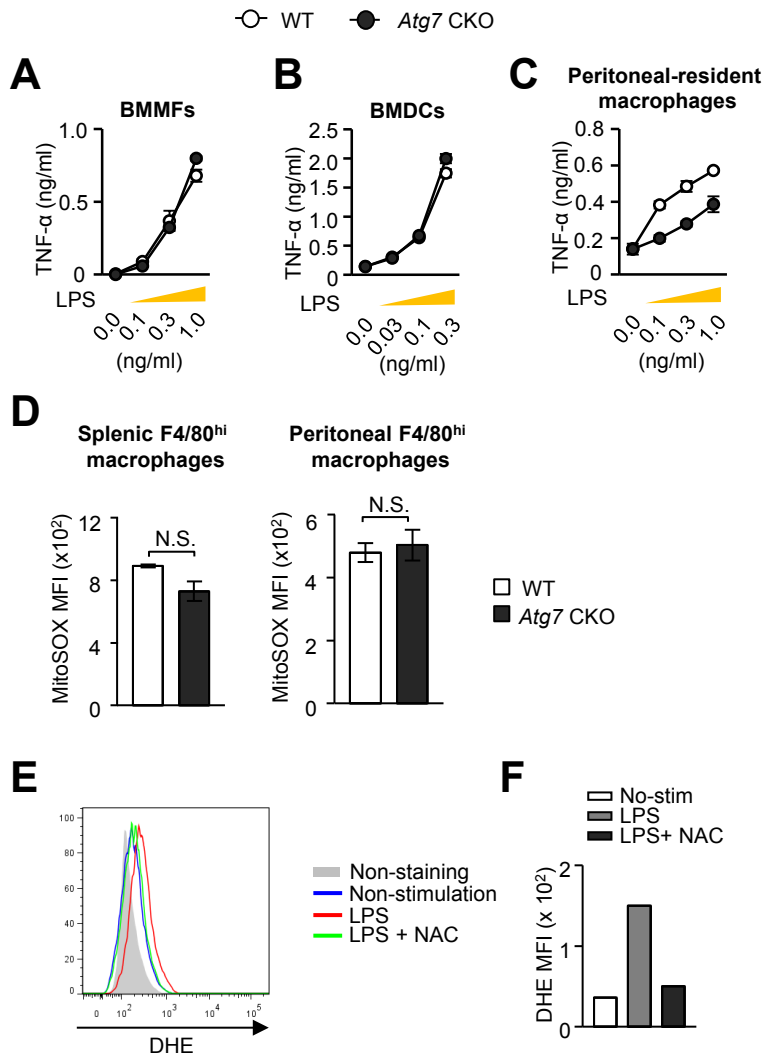
SUPPLEMENTARY FIGURE 2. Histological evaluation and therapeutic efficacy of antibiotics in drinking water for pulmonary inflammation in *Atg7* CKO mice. (A) Representative images of lung sections obtained from WT and *Atg7* CKO mice. Scale bar indicates 100 μ m. (B) Measurement of air sacculae areas was performed from lung sections stained with H&E. Multiple measurements were performed on randomly selected 0.63-mm² fields (5 fields per mouse) located in the distal part of the lung sections. The proportion of lung comprising terminal saccular spaces was calculated as a percentage of the total examined area of the lung section. Six animals per genotype were examined. (C) Pan-bacterial *16S* rRNA levels in spleen, kidney and mesenteric LNs assessed by qPCR with universal bacterial *16S* rRNA primers. RNA were isolated from the lung, spleen, kidney and mesenteric LN of 3-wks old WT and *Atg7* CKO mice. Mouse β -actin mRNA was used as an internal control. $n=3$. (D) Schematic diagram of the experimental protocol. Antibiotics were added in drinking water when mice were set up for breeding. The antibiotics treatment was continued through pregnancy until weaning pups at 3-wk after their birth. Thus, the newborns have been exposed to antibiotics both in pre- and post-natal periods. (E) RNA was isolated from whole lungs of the 3-wk old pups, and *16S* rRNA was assessed by qPCR. (F) Comparison of mRNA levels of *Il6* and *Cxcl1* in the lung between WT and *Atg7* CKO mice with or without antibiotics treatment. Shown are levels of gene expression in *Atg7* CKO mice relative to that in WT mice. A broken line denotes the ratio of “1,” with which *Atg7* CKO and WT lungs express the same levels of mRNA. Error bars represent mean \pm SD. Data are representative of two independent experiments. * $p < 0.05$. N.S.; not significant.

Supplementary Figure 3



SUPPLEMENTARY FIGURE 3. Characterization of AMs and cDCs in the lung. (A, B) CD11b expression on the surface of AMs. AMs were gated as CD45⁺CD11c^{hi}F4/80⁺, and their CD11b expression levels were compared between 7-wk old WT and *Atg7* CKO (A). Mean fluorescence intensity (MFI) of CD11b expression was statistically analyzed (B). (C) Comparison of CD11b expression levels on AMs between WT and *Atg7* CKO mice. Shown are values of MFI on AMs from *Atg7* CKO AMs relative to that from WT mice. (D) MFI of CD11c and F4/80 staining intensity on the surface of AMs obtained from 7-wk old WT and *Atg7* CKO mice. (E) Granularity shown as side-scatter (SSC-A) and cell size as forward-scatter (FSC-A) in *Atg7*-deficient and *Atg7*-sufficient AMs. (F) MFI of CD11c expression on the surface of cDC in the lung of 7-wk old WT and *Atg7* CKO mice. (G) Granularity and cell sizes of *Atg7*-deficient and *Atg7*-sufficient cDCs in the lung. (H) AMs from 17-day old *Atg7* CKO and WT mice were analyzed by flow cytometry to evaluate MFI of indicated receptors. $n=3$. Error bars represent mean \pm SD. Data are representative of at least two independent experiments. *; $p < 0.05$. N.S.; not significant.

Supplementary Figure 4



SUPPLEMENTARY FIGURE 4. Lack of *Atg7* in BMDMs, BMDCs, peritoneal macrophages, and splenic macrophages does not induce cell sensitivity towards low levels of LPS and ROS production. (A-C) BMDMs (A) and BMDCs (B) were generated from BM of 7-wk old mice, and peritoneal-resident macrophages (C) were obtained from 2-wk old WT and *Atg7* CKO mice. Indicated cells ($2.5 \times 10^5/\text{ml}$) were stimulated with LPS (0-1 ng/ml) for 24 hrs and TNF- α production in the supernatants were evaluated by ELISA. (D) Mitochondrial ROS production in splenic-resident and peritoneal-resident macrophages. Cells were harvested from 2-wks old WT and *Atg7* CKO mice as of F4/80^{hi}. Production of mtROS was evaluated by MitoSOX. $n=3$ per group. Error bars represent mean \pm SD. (E, F), RAW-blue cells were stimulated with LPS (100ng/ml) in the presence or absence of NAC (10mM) for 24 hr. Production of ROS was evaluated by DHE. MFI of DHE was shown in F. Data are representative of at least two independent experiments.